Crystallographic Study of the Recombinant Flavin-Binding Domain of Baker's Yeast Flavocytochrome b_2: Comparison with the Intact Wild-Type Enzyme†

L. M. Cunane,‡ J. D. Barton,‡ Z.-W. Chen,‡ F. E. Welsh,§ S. K. Chapman,§ G. A. Reid,|| and F. S. Mathews*,‡

Department of Biochemistry and Molecular Biophysics, Washington University School of Medicine, St. Louis, Missouri 63110, Department of Chemistry, University of Edinburgh, West Mains Road, Edinburgh, EH9 3JJ, U.K., and Institute of Cell and Molecular Biology, University of Edinburgh, Mayfield Road, Edinburgh, EH9 3JR, U.K.

Received October 30, 2001; Revised Manuscript Received January 28, 2002

ABSTRACT: Flavocytochrome b_2 catalyzes the oxidation of L-lactate to pyruvate and the transfer of electrons to cytochrome *c*. The enzyme consists of a flavin-binding domain, which includes the active site for lacate oxidation, and a b_2-cytochrome domain, required for efficient cytochrome *c* reduction. To better understand the structure and function of intra- and interprotein electron transfer, we have determined the crystal structure of the independently expressed flavin-binding domain of flavocytochrome b_2 to 2.50 Å resolution and compared this with the structure of the intact enzyme, redetermined at 2.30 Å resolution, both structures being from crystals cooled to 100 K. Whereas there is little overall difference between these structures, we do observe significant local changes near the interface region, some of which impact on amino acid side chains, such as Arg289, that have been shown previously to have an important role in catalysis. The disordered loop region found in flavocytochrome b_2 and its close homologues remain unresolved in frozen crystals of the flavin-binding domain, implying that the presence of the b_2-cytochrome domain is not responsible for this positional disorder. The flavin-binding domain interacts poorly with cytochrome *c*, but we have introduced acidic residues in the interdomain interface region with the aim of enhancing cytochrome *c* binding. While the mutations L199E and K201E within the flavin-binding domain resulted in unimpaired lactate dehydrogenase activity, they failed to enhance electron-transfer rates with cytochrome *c*. This is most likely due to the disordered loop region obscuring all or part of the surface having the potential for productive interaction with cytochrome *c*.

Flavocytochrome b_2 (L-lactate:cytochrome *c* oxidoreductase, EC 1.1.2.3) from *Saccharomyces cerevisiae* (FCB2)[1] catalyses the oxidation of L-lactate to pyruvate with a subsequent transfer of electrons to cytochrome *c* (*1*). It is an important respiratory enzyme located in the intermembrane space of yeast mitochondria where its production is induced by the presence of oxygen and, more specifically, L-lactate. In addition to providing pyruvate (the product of lactate oxidation) for the Krebs cycle, FCB2 also participates in a short electron-transport chain involving cytochrome *c* and cytochrome oxidase. This ultimately directs the reducing equivalents gained from L-lactate oxidation to oxygen, yielding one molecule of ATP for every L-lactate molecule consumed.

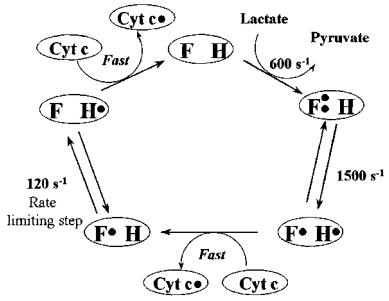

FIGURE 1: Catalytic cycle for FCB2: F, flavin; H, heme; Cyt *c*, cytochrome *c*. Black dots represent electrons; thus, F with two dots is fully reduced flavin, F with one dot is flavin semiquinone, and H with one dot is reduced heme. The rate constants shown are at 25 °C (pH 7.5) and $I = 0.10$ M.

The enzyme is a homotetramer with a subunit molecular mass of 57.5 kDa and contains two noncovalently bound cofactors, FMN and heme, per subunit (*2*). Each subunit is composed of two domains, an N-terminal 11 kDa b_2-cytochrome domain and a C-terminal 45 kDa flavin-binding domain, which are connected by a short, flexible hinge peptide connecting residues Pro99 and Gly100 (*3*). In its physiological reaction, two electrons are transferred from the substrate-reduced flavin ring to cytochrome *c* via two one-electron transfer events mediated by the b_2-cytochrome domain involving transient formation of a flavin semiquinone (Figure 1).

† This work was supported by NIH Grant No. GM-20530 (F.S.M.), by the U.K. Biotechnology and Biological Sciences Research Council (S.K.C., G.A.R., and F.E.W.), and by the Wellcome Trust funded Edinburgh Protein Interaction Centre (EPIC). Use of the Advanced Photon Source was supported by the U.S. Department of Energy, Basic Energy Sciences, Office of Science, under Contract No. W-31-109-Eng-38.

* Corresponding author. Phone: (314) 362-1080. Fax: (314) 362-7183. E-mail: mathews@biochem.wustl.edu.

‡ Washington University School of Medicine.

§ Department of Chemistry, University of Edinburgh.

|| Institute of Cell and Molecular Biology, University of Edinburgh.

[1] Abbreviations: FCB2, flavocytochrome b_2; FBD, flavin-binding domain of flavocytochrome b_2; L199E-FBD, leucine199 → glutamate mutation in FBD; K201E-FBD, lysine201 → glutamate mutation in FBD; NCS, noncrystallographic symmetry.

10.1021/bi0119870 CCC: $22.00
Published on Web 03/08/2002

Several attempts have been made to separate the domains by proteolysis of the intact enzyme (*4*−*6*), and the b_2-cytochrome domain has been successfully isolated after tryptic digestion. The flavin-binding domain of FCB2, however, is difficult to isolate by proteolytic methods, mainly because of a region within the domain that is highly protease sensitive (*7*).

The gene for FCB2 has been cloned and the enzyme expressed at high levels in *Escherichia coli* (*8*). In addition, the flavin-binding domain (FBD) of flavocytochrome b_2 has been expressed independently in *E. coli* (*9*). The independent FBD is an efficient L-lactate dehydrogenase when ferricyanide is the electron acceptor. However, it shows virtually no reductase activity toward cytochrome *c*, the physiological electron acceptor for the intact enzyme. Electron transfer from FBD to the separately expressed b_2-cytochrome domain is essentially undetectable (*9*). Furthermore, FBD has very poor oxidase activity with molecular oxygen (*10*), in contrast to its structural homologue, glycolate oxidase, which utilizes dioxygen as its primary electron acceptor.

The structural analysis of FBD was undertaken, primarily, to investigate whether a disordered loop (299−317) in FCB2 close to the active site and to the interaction site for the b_2-cytochrome domain might be stabilized. The structure of FBD was used as a basis to attempt the construction of a cytochrome *c* binding site on the FBD surface, and the kinetic characterization of two mutant forms of FBD, with this aim in mind, is reported. A new structural model of native FCB2 is also reported, refined to 2.30 Å resolution against a recent low-temperature X-ray data set, thereby serving as an improved benchmark against which the structural features of the recombinant flavin-binding domain may be compared.

MATERIALS AND METHODS

DNA Manipulation, Strains, Media, and Growth. FBD was expressed and isolated as previously described (*9*). The mutant enzymes L199E-FBD and K201E-FBD were generated by site-directed mutagenesis using the method described by Kunkel and Roberts (*11*). The mutagenic oligonucleotides GCTACAGCTGAGTGTAAACTGG (which substitutes leucine199 with glutamate) and GCTTTGTGTGAACTGGGAAACC (which substitutes lysine201 with glutamate) were used. Mismatched bases are underlined. The mutated FBD coding regions were fully sequenced from single-stranded DNA to verify that no secondary mutations had been introduced. The two mutant forms of FBD were expressed in *E. coli* strain TG1 using the expression vector pRC23, as previously described (*9*). Standard methods for the growth of *E. coli*, plasmid purification, DNA manipulation, and transformation were performed as described in Sambrook et al. (*12*).

Protein Purification and Kinetic Analysis. FBD, L199E-FBD. and K201E-FBD were purified using the previously reported protocol for FBD (*9*). Steady-state kinetic experiments were performed at 25 °C in Tris-HCl (pH 7.5) and *I* at 0.10 M. Buffer concentration was 10 mM in HCl with *I* adjusted to 0.10 M by the addition of NaCl. The L-lactate-dependent reduction of ferricyanide (potassium salt, BDH) was monitored by the decrease in absorbance at 420 nm ($\epsilon = 1010\ M^{-1}\ cm^{-1}$) using a Shimadzu 2101 spectrophotometer. A saturating concentration of ferricyanide (2 mM) was used in all assays. The L-lactate-dependent reduction of cytochrome *c* (horse, Sigma type VI) was followed by the increase in absorbance at 550 nm using published absorption coefficients for reduced and oxidized forms (*13*). Concentrations of FBD were determined as reported elsewhere (*9*). L-Lactate concentration dependences were determined over the range of 0.05−100 mM. Cytochrome *c* concentration dependences were determined over the range of 0.1−100 μM.

Wild-type FCB2 was prepared from commercially available lyophilized bakers yeast, as described in the literature (*2*).

Kinetic parameters k_{cat} and K_m were determined from steady-state results using nonlinear regression analysis (Microcal Origin software).

Crystallography. Crystals of recombinant FBD were grown by the hanging-drop vapor diffusion method. Three microliters of a protein solution (at 10 mg/mL in 0.1 M Tris buffer (pH 7.5)) was mixed with 3 μL of a reservoir solution (26% PEG 4K, 0.17 M sodium citrate (pH 5.6), and 3% ethylene glycol) and allowed to equilibrate at 4 °C. The crystals were yellow, confirming that they were in the oxidized state. Data were recorded to 2.5 Å resolution from a very small (0.05 × 0.05 × 0.20 mm) frozen FBD crystal (soaked 1 min in 30% PEG 4K, 0.17 M citrate (pH 5.6) and 3% ethylene glycol) at the Structural Biology Center beam-line 19-ID of the Advanced Photon Source, Argonne National Laboratory, Argon, IL. The crystals are orthorhombic, space group $P2_12_12$, $a = 110.7$ Å, $b = 147.6$ Å, $c = 64.8$ Å, and contain 2 subunits in the asymmetric unit. The data were processed with HKL2000 (*14*), resulting in $R_{merge} = 8.3\%$. Data collection statistics are summarized in Table 1.

Crystals of native FCB2 were grown by microdialysis, as described previously (*15*). The protein solution (5−7.5 mg/mL in a 50 mM phosphate buffer (pH 7.2), 50 mM D,L-lactate, and 1 mM EDTA) was dialyzed at 4 °C in capillary tubes (10 × 3 mm) sealed by a dialysis membrane, against 30−33% (v/v) 2-methyl-2,4-pentanediol (MPD), 70 mM phosphate buffer (pH 7.2), 47 mM D,L-lactate, and 1 mM EDTA. Data were collected to 2.3 Å resolution using an R-Axis IV image-plate system from an FCB2 crystal (0.3 × 0.3 × 0.5 mm) flash-cooled directly from the mother liquor. The crystals are trigonal, space group $P3_221$, $a = b = 164.2$ Å, $c = 111.6$ Å, with 2 subunits in the asymmetric unit. The data set was processed with DENZO (*16*) and SCALEPACK (*16*), merging to $R_{merge} = 4.3\%$ (see Table 1).

A clear solution to the structure of the recombinant FBD was obtained by the molecular replacement method with the program AMoRe (*17*), using the flavoprotein domain of flavocytochrome b_2 (Protein Data Bank ID, 1fcb) (*3*) as the search model. Structure refinements were initiated with X-PLOR, version 3.843 (*18*), in the resolution range of 6.0−3.0 Å and continued with CNS, version 1.0 (*19*), using all data to 2.5 Å. In the case of FCB2, the unit cell dimensions of the cryogenically cooled native crystals were very similar to those of the room-temperature crystals determined previously (1fcb) (*3*) allowing for direct refinement starting with the atomic model. The FCB2 refinements were performed first with X-PLOR, version 3.843 (*18*), using data in the range of 6.0−2.3 Å resolution and subsequently with CNS, version 1.0 (*19*), using all data to 2.3 Å.

Table 1: Data Collection and Refinement Statistics for Recombinant Flavin-Binding Domain (FBD) and Wild-Type Flavocytochrome b_2 (FCB2)

data collection	FBD	FCB2
resolution (all/outer)(Å)	50.00−2.50/2.54−2.50	40.00−2.30/2.34−2.30
no. of observed reflections	240 788	157 962
no. of unique reflections	36 688	65 248
completeness (all/outer)(%)	98.8/96.2	90.5/73.7
R_{merge} (all/outer)(%)[a]	0.083/0.345	0.043/0.207
$<I/\sigma(I)>$ (all/outer)[b]	21.3/5.2	25.6/4.8
redundancy (all/outer)	6.6/5.8	2.2/1.6
	Refinement	
resolution (Å)	40.0−2.5	30.0−2.3
R[c]	0.157	0.170
R_{free}[c,d]	0.203	0.211
no. of protein atoms (non-H)	6120	7056
no. of solvent molecules	370	618
no. of FMN	2	2
no. of Heme	0	1
no. of ethylene glycol	2	0
no. of pyruvate	0	1
no. of MPD	0	5
no. of phosphate ions	0	1
no. of res. in alternate conformation	6	4
$<B>$(all atoms) (Å^2)	38	36
rms ΔB (main chain−main chain) (Å^2)	1.9	1.8
rms ΔB (side chain−side chain) (Å^2)	3.5	2.9
rms deviation, bond lengths (Å)	0.010	0.011
rms deviation, bond angles (deg)	1.6	1.9

[a] $R_{merge} = \sum_h \sum_i |I(h) - I_i(h)| \sum_h \sum_i I_i(h)$, where $I_i(h)$ and $I(h)$ are the ith and mean measurement of reflection h. [b] $I/\sigma(I)$ is the average signal-to-noise ratio for merged reflection intensities. [c] $R = \sum_h |F_o - F_c| / \sum_h F_o$, where F_o and F_c are the observed and calculated structure factor amplitudes of reflection h. [d] R_{free} is the test reflection data set, about 10% selected randomly for cross validation during crystallographic refinement (*20*).

Both structures were refined with essentially the same protocols. All data were used in the CNS refinements, except for 10% set aside for cross-validation (R_{free}) (*20*). The refinements included a correction for bulk solvent. The non-crystallographic symmetry (NCS) between the two flavoprotein monomers in the asymmetric unit of both crystal types was utilized, starting with NCS constraints (for FBD) or very strong restraints (for FCB2); the NCS restraints were later extended to both proteins, relaxed, and validated with R_{free}. Refinement with simulated annealing was employed at the outset to remove any bias from the starting models and also when transferring the refinements from X-PLOR to CNS. The structures were rebuilt, using TURBO−FRODO (*21*), in $2F_o - F_c$ electron-density maps with some help from $3F_o - 2F_c$ maps, in an attempt to interpret the regions with weak density. Water molecules were added at the 3σ level in $F_o - F_c$ maps, and those which refined to high-temperature factors ($B > 50$ Å^2) were removed from the model. In the later stages of refinement, NCS restraints were removed from a small number of isolated residues or small segments of polypeptide chain where disorder remained evident in the electron-density maps, as a result of alternate side-chain conformations, or in regions that had been difficult to interpret. Refinement statistics are summarized in Table 1.

Selection of Mutant Constructs of FBD for Kinetic Analysis. The cytochrome *c* structure was, first, manually docked onto the surface of the isolated flavin domain. The constraints on these preliminary docking experiments were such that the heme of cytochrome *c* and the flavin group of FBD should be less than 14 Å apart. This dramatically limits the number of possible models. No water molecules were included in any of the modeling experiments. Trial docking refinements were carried out using the program XPLOR (*18*). The best results for minimizing the heme-to-flavin distance suggested that L199 and K201 were major impediments to the formation of a reasonable complex between cytochrome *c* and FBD. These residues were therefore chosen for mutagenesis experiments.

RESULTS AND DISCUSSION

Structure of the Recombinant Flavin-Binding Domain (FBD). The final model of FBD includes residues 100−298 and 318−511 in subunit A and 100−297 and 318−511 in subunit B. (In native flavocytochrome b_2, residues 1−99 are the b_2-cytochrome domain, which is not present in the FBD construct.) The segment of polypeptide chain between 298 and 318 is not visible in the electron-density maps, as was the case in the original native flavocytochrome b_2 structure (*3*), and this was attributed to it being a mobile, disordered loop. This loop is located on the protein surface and is extremely sensitive to protease activity. Several residues have alternative side-chain conformations: Glu236, Arg289, Met460, and Asp476 in subunit A and Asp182 and Asp476 in subunit B. The NCS relationship between the two monomers in the asymmetric unit was applied with strong restraints on the main-chain atoms and weaker ones on the side chains, leading to an rms deviation among all C_α atoms of 0.09 Å when subunits A and B are compared. The only significant difference between the main chains of subunits A and B appears just beyond the C-terminal end of the disordered loop, in residues 318−325. A trio of "second tier" active-site residues, Leu286, Arg289, and Asp292, differ between subunits A and B; in subunit A they are well-ordered, but in B, their side chains reside in weaker density, have higher *B* values, and adopt somewhat different conformations. The principal active-site residues, Tyr143,

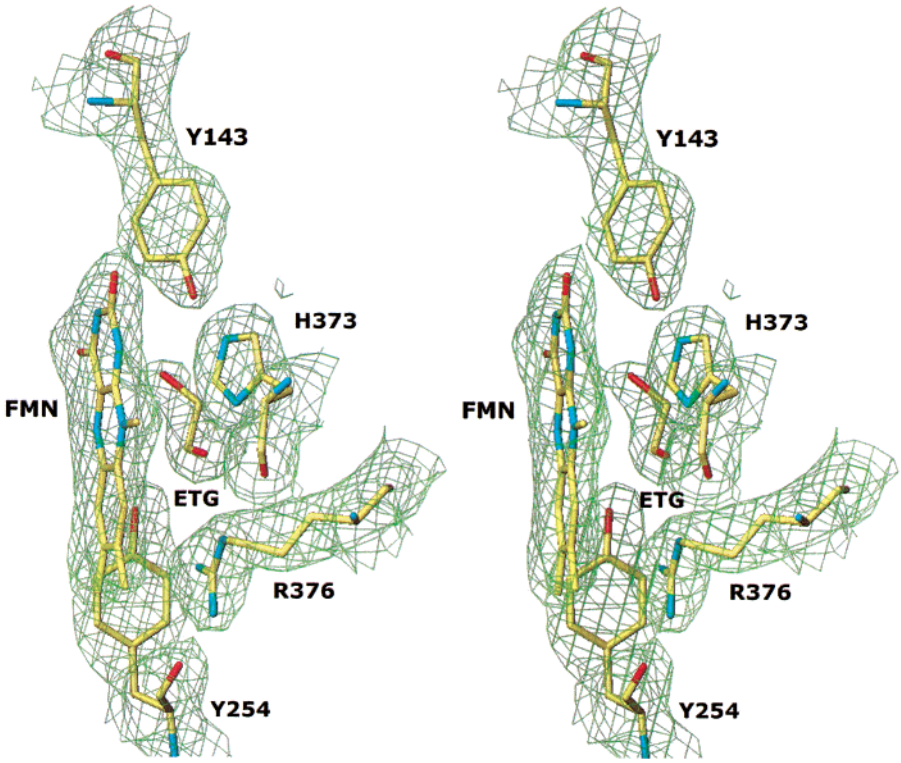

FIGURE 2: Electron density in the active site of one of the FBD subunits (contoured at the 1.2 σ level). The principal active-site residues and cofactor FMN are depicted, and the bound ethylene glycol molecule is shown, mimicking substrate binding in native flavocytochrome b_2. This diagram was prepared using TURBO−FRODO (*21*).

Tyr254, His373, and Arg376, match almost exactly when the two subunits are superimposed.

The FBD model also contains the FMN cofactor bound in each subunit, 370 water molecules, and an ethylene glycol molecule (Figure 2) bound in the active site of each subunit. The presence of ethylene glycol bound in the active site, which is accessible to the ligand, is not surprising given that substrate was not present in the crystal growth medium, whereas ethylene glycol was, and that the latter is very similar in size and chemical properties to the substrate, lactate. In fact, ethylene glycol could be considered an accidental substrate analogue. One of the ethylene glycol hydroxyl groups makes hydrogen-bond interactions with Arg376 and Arg289 and the other with Tyr254 and the FMN O4 atom. The interaction of ethylene glycol with Arg289 is consistent with the recently confirmed role of Arg289 in catalysis (*22*, *23*).

Structure of Native Flavocytochrome b_2 (FCB2). The final model of FCB2 contains residues 1−300 and 308−511 in subunit A and 99−300 and 309−511 in subunit B. In subunit A, Glu104, Gln288, Lys324, and Asn492 are modeled with alternative side-chain conformations. As in the original room-temperature flavocytochrome b_2 structure, only one b_2-cytochrome domain was found per asymmetric unit (i.e., 2 b_2-cytochrome domains per FCB2 tetramer). Some significant electron density was visible in the region where the subunit B b_2-cytochrome might be located, but it was weak, discontinuous, and uninterpretable. The model of FCB2 also contains a well-ordered heme in the observable b_2-cytochrome domain, FMN in each flavin-binding domain, 618 water molecules, five molecules of MPD bound at the protein surface, and a phosphate ion located on the molecular 4-fold symmetry axis of the tetramer. A persisting electron-density feature in the active site of subunit B was modeled with a pyruvate ion (the reaction product), as had been done previously in the original flavocytochrome b_2 structure. The pyruvate−protein contacts are with Arg376, Tyr143, Tyr254, and His373. In subunit A, a network of well-ordered water molecules fills the substrate-binding site. The average temperature factor in the visible b_2-cytochrome domain is 62 Å^2, much higher than that in the flavin domains, where the average B value is 33 Å^2, indicating the generally higher mobility of the b_2-cytochrome domain, which is not unexpected given that it packs on the outside of the tightly self-associated flavoprotein tetramer (*3*).

The FCB2 structure is very similar to the room-temperature structure, 1fcb, determined earlier. The differences probably represent improvements in the model that have resulted from increased resolution, collection of data at low temperature, and calculation of "error-weighted" electron-density maps (*24*). In FCB2, several more residues were located in the loop that was disordered in 1fcb (residues 300−316 and 300−311 in the two subunits), reducing the extent of the disorder to seven or eight residues (Figure 3). A helical segment between the heme and flavin domains, residues 102−115, was rebuilt leading to a shift in register. In addition, a number of side chains are more clearly defined, resulting in identification of two hydrogen bonds between the flavin and b_2-cytochrome domains in addition to the seven found earlier (*3*) and a shortening to 2.7 Å from 3.3 Å of the hydrogen bond between a heme propionate (OD1) and Lys296 (NZ). The active-site water molecules in subunit A are retained, as is the pyruvate molecule in subunit B, although the latter was not restrained to be planar (as it was in 1fcb) and has subsequently refined to about 47° away from planarity. Attempts to restrain pyruvate to being planar in

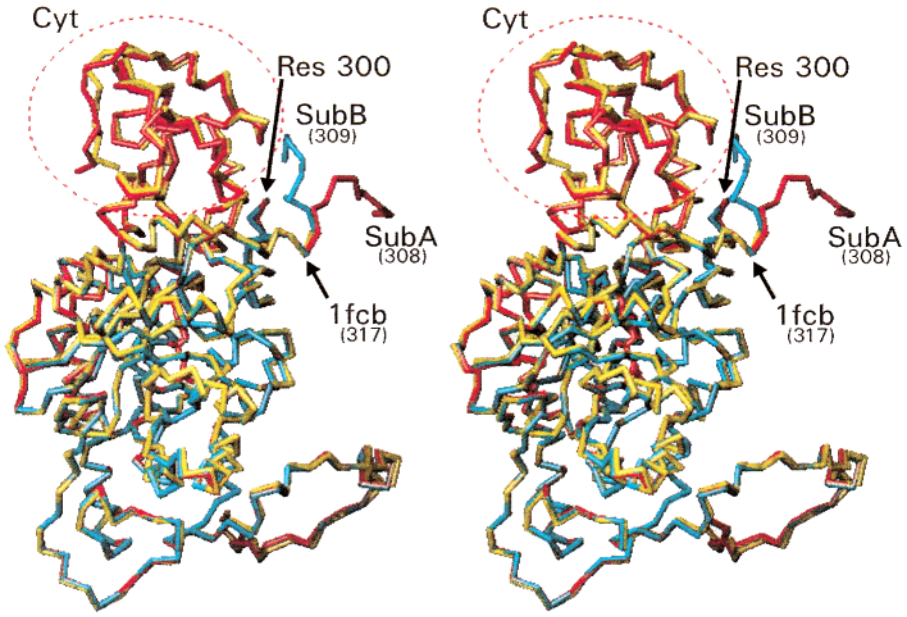

FIGURE 3: Superimposed C_α traces of flavocytochrome b_2. The original room-temperature structure (1fcb, subunit A) is shown in yellow, and the A and B subunits of FCB2 are shown in red and aqua, respectively. The start of the disordered loop region, residue 300, is indicated as are the extents to which this loop region could be fitted to electron density in each of the three models. In FCB2, several more residues were found than in 1fcb, and they follow different paths in subunits A and B, correlating with the presence or absence of the b_2-cytochrome domain. The b_2-cytochrome domain, observed in only subunit A of FCB2 and the 1fcb structure, is circled in red. This diagram was prepared using TURBO−FRODO (*21*).

FCB2 led to significant features in difference electron-density maps indicative of a nonplanar conformation for pyruvate. The only real difference in conformation seems to be a slight rearrangement of the first 10 amino acids of the cytochrome domain that might result from small differences in crystal packing caused by an approximately 3.5% shrinkage in the unit cell volume.

A comparison between the flavoprotein domains of FCB2 gives an rms deviation of 0.10 Å for 95% of the C_α atoms. The largest structural difference between the two subunits occurs just beyond the mobile loop regions (residues 301−307 and 301−308, respectively) at the point of resumption of the ordered structure, where the residues from positions 317 to 309 follow divergent paths (Figure 3); in subunit B, the polypeptide encroaches into the space which would be occupied by the b_2-cytochrome were it ordered. Smaller differences between the two subunits occur in five other regions. One of these is the N-terminal portion of the flavoprotein domain of FCB2, residues 99−115; the *B* values of this stretch are considerably higher in the B subunit (average $B = 67$ Å^2) than in subunit A (average $B = 50$ Å^2), consistent with the very high disorder of the b_2-cytochrome domain. A second region is in the vicinity of Gln139, which lies adjacent to the hinge peptide and makes a hydrogen bond to the heme propionate group in subunit A. A third region, similarly affected by the proximity of the ordered cytochrome domain, is found around Leu199, which in subunit A is in van der Waals contact with the heme. A fourth region, Leu286, which projects into the active-site pocket, has different side-chain orientations in the two subunits, with the CD1 and CD2 atoms pointed in toward the bound pyruvate in the active site of subunit B. Finally, Phe325 shows evidence of disorder in subunit B and adopts a different conformation from A, where it makes several van der Waals contacts with the b_2-cytochrome domain and the heme. Clearly, most of the differences cited here are a consequence of the absence of an ordered b_2-cytochrome domain in subunit B. In contrast, the principal active-site residues Tyr143, Tyr254, His373, and Arg376 match closely when the two subunits are superimposed.

Comparison between FBD and FCB2. The recombinant flavin-binding domain crystallizes in a space group different from FCB2, most likely because of the absence of the b_2-cytochrome domain. The FBD subunits pack together as a tetramer in exactly the same manner as in FCB2, although there are different intermolecular contacts between tetramers in the crystal. An alignment of the flavoprotein dimers of FBD and FCB2 reveals that, for all of the C_α atoms (100−511), the rms deviation between the two structures is 0.36 Å and reduces to 0.16 when C_α pairs differing by greater than 2 Å are omitted. The most prominent differences occur in the region of the disordered loop (see the following discussion) and in a turn located at the protein surface (residues 394−403), which in FBD has close crystal contacts but in FCB2 does not; the latter has higher *B* values and weaker electron density than its surroundings.

In FBD, the "substrate analogue" ethylene glycol is bound at the active site of both subunits. In FCB2, the pyruvate molecule binds only in subunit B, in which the b_2-cytochrome domain is disordered, while subunit A has its active site filled with water molecules. The solvent accessibility of the flavin ring in the two structures is nearly the same.

As expected, the catalytic site for lactate oxidation in FBD is virtually unchanged. Only the side-chain orientation of Tyr143 differs slightly between the two structures (Figure 4). Several residues close to the active site, however, show more marked differences between FCB2 and FBD. Arg289, recently demonstrated to be important for catalysis in FCB2 (*22*, *23*), exists in two conformations in FBD but takes up only a single conformation in native FCB2 (Figure 4). In

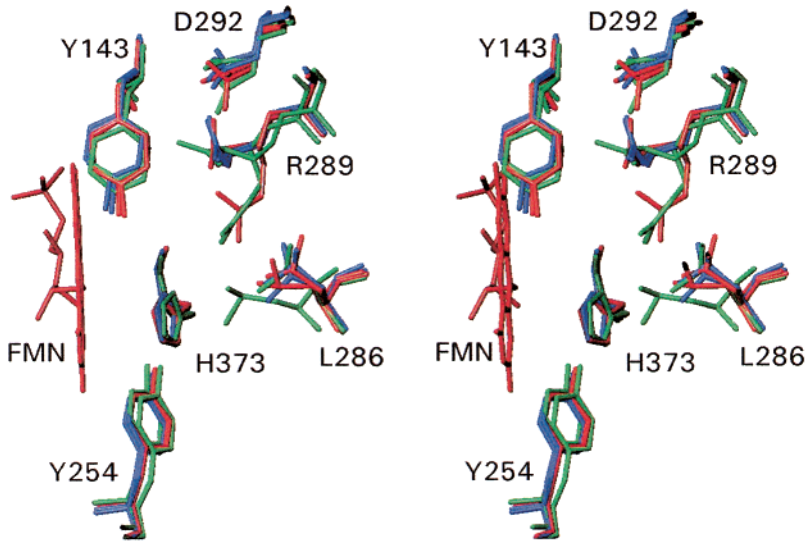

FIGURE 4: Stereoview of the region in flavocytochrome b_2 near Arg289 that exhibits considerable flexibility among several crystal structures. Superimposed are FBD (red) and FCB2 (blue) from this study and 1LDC, a Tyr143Phe mutant of flavocytochrome b_2 containing lactate bound at the active site (green). In the Arg289 region, most flavocytochrome b_2 structures find Arg289 oriented away from the substrate cavity (distal orientation) and making a hydrogen bond with Asp292. In a few of the structures, however, Arg289 points toward the substrate binding site (the proximal orientation) and interacts with a glutamine side chain (Gln377, not shown). In FBD subunit A, Arg289 exists in either of these conformations; in subunit B of FBD, Arg289 exists only in the proximal orientation; in the Tyr143Phe mutant with lactate bound, one subunit has Arg289 in the proximal orientation and the other in the distal conformation. This diagram was prepared using TURBO−FRODO (*21*).

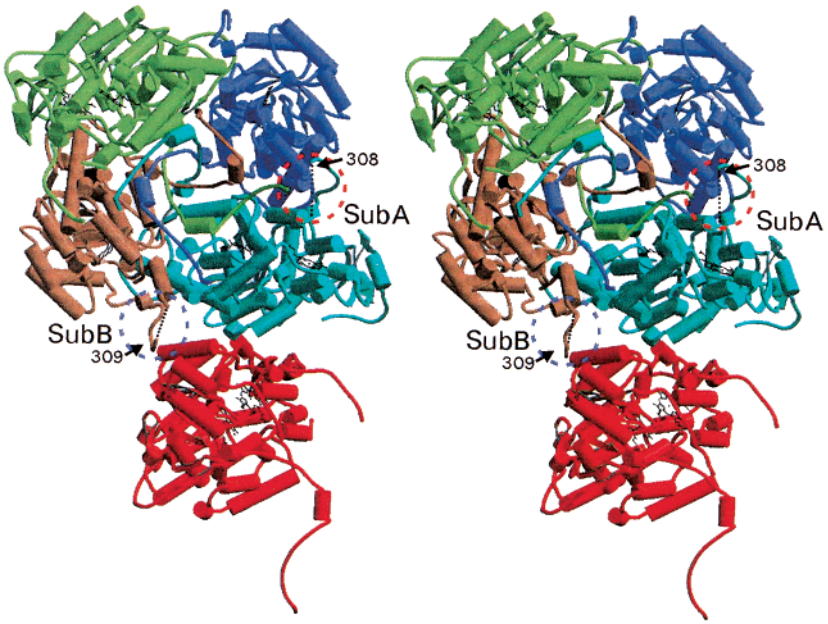

FIGURE 5: Packing differences between subunits A and B of FCB2 in the region of the disordered loop. The subunits of the crystallographic FCB2 dimer are shown in aquamarine and magenta, respectively, and symmetry-related dimer subunits in green and blue. In subunit A, the C-terminal end of the loop (circled in red) folds away from the cytochrome and packs against subunit B′ of the 2-fold symmetry-related dimer of the same FCB2 tetramer. In subunit B (circled in blue), the same segment of loop extends into the region where cytochrome would be, were it ordered, and packs against a segment of an adjacent tetramer, one subunit of which is shown in red. The ends of the disordered loops in subunits A and B are joined by dashed lines, and residues 308 and 309 are labeled. This diagram was made using MOLSCRIPT (*33*) and RASTER3D (*34*).

FBD, one of the Arg289 conformers makes a contact with ethylene glycol, whereas, in FCB2, the guanidinium group does not interact with pyruvate. In a Tyr143Phe mutant of recombinant FCB2 which contains lactate bound at the active site (*25*), Arg289 also exists in two conformations. It appears that the orientation of Arg289 is sensitive to the species that is bound in the active site, supporting its proposed role in catalysis. Asp292 also takes up different positions in FCB2 and FBD, correlating with the placement of Arg289, with which it makes a hydrogen bond. The Leu286 side chain has a different rotational conformer in each of the four subunits (A and B in FCB2 and FBD; Figure 4) suggesting an inherent flexibility, which may be necessary given its proximity to the adaptable Arg289 side chain.

The region of FBD that would form the interface with the b_2-cytochrome domain is generally closer in conformation

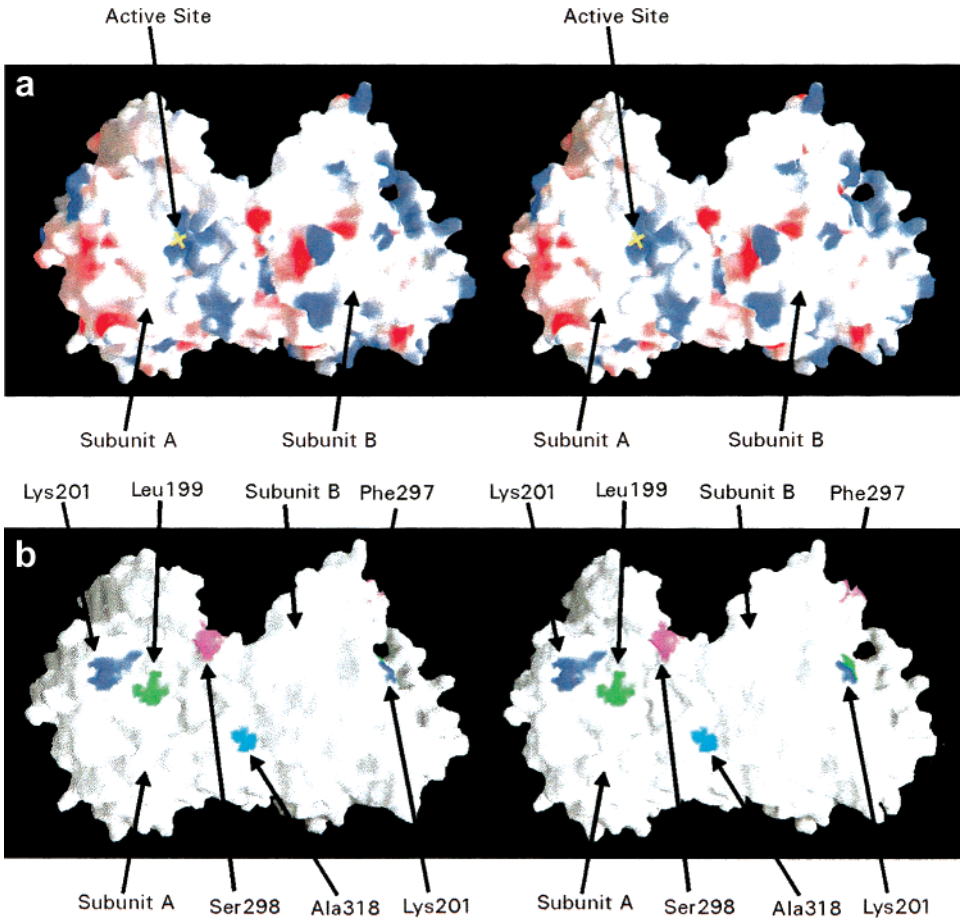

FIGURE 6: Stereoview of the molecular surface of FBD showing two subunits, A and B, that are related by 90° rotation about an axis that is roughly vertical. (a) The active site in subunit A, where the flavin has maximal solvent exposure and would be the most favorable interaction site for efficient electron transfer to cytochrome *c*, is indicated by a yellow cross. The surface is colored by electrostatic potential with blue (positive), red (negative), and white (neutral). The active site in subunit B is not visible. (b) Molecular surface viewed in the same orientation as part a, with residues Leu199 and Lys201 of subunit A highlighted in green and dark blue, respectively. The two end-points of the disordered loop between Ser298 and Ala318 in subunit A are highlighted in violet and light blue, respectively. Two of these residues, Lys201 and Phe297 (replacing Ser298), in subunit B are also highlighted. The remainder are not easily visible because of the 90° rotation of subunit B. This diagram was prepared using the program GRASP (*35*).

to subunit B of FCB2, where b_2-cytochrome is disordered, than to subunit A, where b_2-cytochrome domain is ordered. It does not seem likely that the small differences observed between FBD and FCB2 subunit A at the interface could prevent effective binding of the separately expressed b_2-cytochrome domain to FBD because these changes are probably induced by the binding of the b_2-cytochrome domain. The physical connection between the b_2-cytochrome domain and the flavin domain in FCB2 seems to be a key factor in the lack of complex formation between the separately expressed domains. It has been previously demonstrated that the sequence and length of the nine-residue segment preceding the hinge peptide have optimally evolved for efficient catalysis in flavocytochrome b_2 (*26*−*28*).

The removal of the b_2-cytochrome domain appears not to have stabilized the mobile loop (297−318) of the flavin domain at all, because there are fewer residues visible in the electron density in this segment than in either 1fcb or FCB2. This suggests that the mobility of the loop is inherent in the flavin domain and demonstrates that the disorder is not induced by the presence of the b_2-cytochrome. The residues at both ends of the 22-residue disordered region in FBD overlay well in subunits A and B. In FCB2, residues up to position 300 in both subunits are also essentially in the same position, at the end of nonbarrel helix αE about 20 residues beyond strand β4 (see ref *3*). Starting at positions 308 and 309, however, the residues following the disorder take up quite different paths (Figure 3). In the A subunit, residues 308−316 extend well away from the bound b_2-cytochrome, with Gly308 packed against Tyr442 of subunit B′ (where B′ indicates a crystallographic symmetry related subunit) of the same tetramer (which is between helix βG and helix α8; see ref 3) (Figure 5). In subunit B, these residues are directed toward the region where the b_2-cytochrome would be, were it ordered, with residue Phe309 in van der Waals contact with Lys340 (near the end of helix α4; see ref 3) of an adjacent tetramer that makes contact in the crystal (Figure 5).

Structural Implications for the Interaction of FBD with Cytochrome c. It has been previously shown that FBD behaves as an efficient L-lactate dehydrogenase with ferricyanide as an electron acceptor with a k_{cat} value similar to that seen for FCB2 (*9*). However, FBD shows very little reductase activity toward cytochrome *c* (*9*). Thus, it would appear that the b_2-cytochrome domain of FCB2 is essential for efficient electron transfer to cytochrome *c*. The question

Table 2: Comparison of Steady-State Kinetic Parameters for Wild-Type Flavocytochrome b_2 (FCB2), the Independently Expressed Flavin-Binding Domain (FBD), and the L199E and K201E Mutant Forms of FBD

	ferricyanide as electron acceptor			cytochrome *c* as electron acceptor		
enzyme[a]	k_{cat}, s^{-1}	K_m, mM (lactate)	K_m, mM (ferricyanide)	k_{cat}, s^{-1}	K_m, μM (cytochrome *c*)	k_{cat}/K_m, $M^{-1}\ s^{-1}$
FCB2[b]	400 ± 10	0.49 ± 0.05	$\ll 0.1$	207 ± 10	10 ± 1	2.1×10^7
FBD[c]	273 ± 6	0.22 ± 0.05	0.58 ± 0.06	0.020 ± 0.002	23 ± 7	8.7×10^2
L199E-FBD	30 ± 2	2.0 ± 0.5	0.20 ± 0.04	0.003 ± 0.001	10 ± 2	3.0×10^2
K201E-FBD	250 ± 17	7.2 ± 1.4	0.50 ± 0.05	0.020 ± 0.005	15 ± 5	1.3×10^3

[a] All experiments were carried out at 25 °C in Tris-HCl buffer, pH 7.5 (*I* at 0.10) as described in Materials and Methods. The value of k_{cat} is expressed in moles of electrons transferred per mole of enzyme per second. [b] Data from ref *32*. [c] Data from ref *9*.

arises then, why is FBD a poor reductant for cytochrome *c*? Clearly there is no problem with the driving force because the reduction potential gap between the flavin of FBD ($E_m = -78$ mV (*29*)) and cytochrome *c* ($E_m = +260$ mV (*30*)) is some $^1/_3$ of a volt. A more likely explanation is, therefore, that there is poor recognition between FBD and cytochrome *c*.

It is known that, for efficient electron transfer, cytochrome *c* interacts with its reaction partners using the surface around its exposed heme edge, a surface which is dominated by positively charged residues (*31*). We have examined the FBD crystal structure and have located the surface region of FBD at which the flavin group in the active site has maximum exposure (i.e., the site at which electron transfer to cytochrome *c* would be most favored) (Figure 6a). It appears that this region, near the opening of the flavin-containing active site of the FBD surface is dominated by both hydrophobic and positively charged residues, some of which are highlighted in Figure 6a. This is contrary to what would be expected for a favorable interaction with cytochrome *c*. Therefore, a possible way to improve the reaction between FBD and cytochrome *c* would be to replace hydrophobic and positive residues on the FBD surface by negatively charged residues. Examination of the FBD structure shows that Leu199 and Lys201 are good candidates for such an approach (Figure 6b) (see Materials and Methods). Accordingly, the L199E-FBD and K201E-FBD mutant enzymes were made. The kinetic analysis of these mutant forms are compared to FBD and FCB2 in Table 2.

From Table 2, it can be seen that FCB2, FBD, and the mutant forms of FBD all have reasonable values of k_{cat} for the lactate-dependent reduction of ferricyanide. This indicates that all of these enzymes can function as good L-lactate dehydrogenases. The results for the lactate-dependent reduction of cytochrome *c*, however, show a marked difference between the values of k_{cat} for FCB2 and those for FBD and both FBD-mutant forms. In fact, it is apparent that FCB2 is 10^4-fold more active as a cytochrome *c* reductase than is FBD or the FBD-mutant enzymes. It is also quite clear from Table 2 that the introduction of negative charges on the surface of FBD close to the flavin has not improved the reaction with cytochrome *c*. In fact, in the case of L199E-FBD, there has been a marked decrease in activity with cytochrome *c*, which appears to reflect a similar decrease when ferricyanide is used as electron acceptor (around 8-fold in each case). These data together suggest that there is another, more important, factor influencing the reaction between FBD and cytochrome *c*. An explanation that we favor is that the disordered loop, which is close to this region of the FBD surface (Figure 6b), folds over the area around the most exposed part of the flavin and forms a physical barrier preventing cytochrome *c* from approaching close enough to the flavin for efficient electron transfer to occur. This possibility is supported by rough modeling studies which indicate that the loop would prevent the heme from approaching the flavin by less than ~22 Å. Thus, the L199E and K201E mutations would be ineffective because they too would be covered by the disordered loop. Such a blockage of the exposed flavin ring by the disordered loop of the FBD might also help explain its lack of reactivity with the separately express cytochrome b_2 domain (*9*).

REFERENCES

1. Appleby, C. A., and Morton, R. K. (1954) *Nature 173*, 749−752.
2. Jacq, C., and Lederer, F. (1974) *Eur. J. Biochem. 41*, 311−320.
3. Xia, Z.-x., and Mathews, F. S. (1990) *J. Mol. Biol. 212*, 837−863.
4. Labeyrie, F., Groudinsky, O., Jacquot-Armand, Y., and Naslin, L. (1966) *Biochim. Biophys. Acta 128*, 492−503.
5. Guiard, B., and Lederer, F. (1976) *Biochimie 58*, 305−316.
6. Celerier, J., Risler, Y., Schwenke, J., Janot, J.-M., and Gervais, M. (1989) *Eur. J. Biochem. 182*, 67−75.
7. Ghrir, R., and Lederer, F. (1981) *Eur. J. Biochem. 120*, 279−287.
8. Black, M. T., White, S. A., Reid, G. A., and Chapman, S. K. (1989) *Biochem. J. 258*, 255−259.
9. Balme, A., Brunt, C. E., Pallister, R. L., Chapman, S. K., and Reid, G. A. (1995) *Biochem. J. 309*, 601−605.
10. Reid, G. A., Østergaard, L. H., Goble, M. L., Moysey, R., and Chapman, S. K. (1999) in *Flavins and Flavoproteins* 1999 (Ghisla, S., Kroneck, P., Macheroux, P., and Sund, H., Eds.), pp 405−408, Rudolf Weber, Agency for Scientific Publications, Berlin, Germany.
11. Kunkel, T. A., and Roberts, J. D. (1987) *Methods Enzymol. 154*, 367−382.
12. Sambrook, J., Fritsch, E. F., and Maniatis, T. (1989) Molecular Cloning: A Laboratory Manual, 2nd ed., Cold Spring Harbor Laboratory Press, Plainview, NY.
13. Hazzard, J. T., Cusanovich, M. A., Tainer, J. A., Getzoff, E. D., and Tollin, G. (1986) *Biochemistry 25*, 3318−3328.
14. Otwinowski, Z., and Minor, W. (1997) *Methods Enzymol. 276*, 307−326.
15. Mathews, F. S., and Lederer, F. (1976) *J. Mol. Biol. 102*, 853−857.
16. Otwinowski, Z. (1993) *Proceedings of the CCP4 Study Weekend. Data Collection and Processing* (Sawyer, L. N., Isaacs, N. W., and Bailey, S., Eds.), pp 56−62, Daresbury Laboratory, Warrington, U.K.
17. Navaza, J. (1994) *Acta Crystallogr. A50*, 157−163.
18. Brünger, A. T. (1992) X-PLOR, Version 3.1. A System for crystallography and NMR, Yale University Press, New Haven, CT.

19. Brünger, A. T., Adams, P. D., Clore, G. M., DeLano, W. L., Gros, P., Grosse-Kunstleve, R. W., Jiang, J. S., Kuszewski, J., Nilges, M., Pannu, N. S., Read, R. J., Rice, L. M., Simonson, T., and Warren, G. L. (1998) *Acta Cryst. D54*, 905−921.
20. Brünger, A. T. (1992) *Nature 355*, 472−475.
21. Roussel, A., and Cambillau, C. (1991) TURBO−FRODO, Silicon Graphics Geometry Partners Directory, p 86, Silicon Graphics, Mountain View, CA.
22. Mowat, C. G., Beaudoin, I., Durley, R. C. E., Barton, J. D., Pike, A. D., Chen, Z., Reid, G. A., Chapman, S. K., Mathews, F. S., and Lederer, F. (2000) *Biochemistry 39*, 3266−3275.
23. Sanders, S. A., Williams, C. H., Jr, and Massey, V. (1999) *J. Biol. Chem. 274*, 22289−22295.
24. Read, R. J. (1986). *Acta Crystallogr. A42*, 140−149.
25. Tegoni, M., Begotti, S., and Cambillau, C. (1995) *Biochemistry 34*, 9840−9850.
26. Sharp, R. E., White, P., Chapman, S. K., and Reid, G. A. (1994) *Biochemistry 33*, 5115−5120.
27. Sharp, R. E., Chapman, S. K., and Reid, G. A. (1996) *Biochemistry 35*, 891−899.
28. Sharp, R. E., Chapman, S. K., and Reid, G. A. (1996) *Biochem. J. 316*, 507−513.
29. Ilias, R. M., Sinclair, R., Robertson, D., Neu, A., Chapman, S. K., and Reid, G. A. (1998) *Biochem. J. 333*, 107−115.
30. Moore, G. R., Eley, C. G. S., and Williams, G. (1984) in *Advanced Inorganic Bioinorganic Mechs.* (Sykes, A. G., Ed.), Vol. 3, pp 1−96, Academic Press, London, U.K.
31. Short, D. M., Walkinshaw, M. D., Taylor, P., Reid, G. A., and Chapman, S. K. (1998) *J. Biol. Inorg. Chem. 3*, 246−252.
32. Miles, C. S., Rouviere-Fourmy, N., Lederer, F., Mathews, F. S., Reid, G. A., Black, M. T., and Chapman, S. K. (1992) *Biochem. J. 285*, 187−192
33. Kraulis, P. J (1991) *J. Appl. Crystallogr. 24*, 946−950.
34. Merritt, E. A., and Bacon, D. J. (1997) *Methods Enzymol. 277*, 505−524.
35. Nicholls, A., Sharp, K. A., Honig, B. (1991) *Proteins 11*, 281−296.

BI0119870